Research Paper

THEMED ISSUE: CRevolution 2: Origin and Evolution of the Colorado River System II

GEOSPHERE

GEOSPHERE, v. 17, no. 6

https://doi.org/10.1130/GES02419.1

13 figures; 1 supplemental file

CORRESPONDENCE: spencer7@email.arizona.edu

CITATION: Spencer, J.E., Constenius, K.N., Dettman, D.L., and Domanik, K.J., 2021, Identification of seasonal varves in the lower Pliocene Bouse Formation, lower Colorado River Valley, and implications for Colorado Plateau uplift: Geosphere, v. 17, no. 6, p. 1745–1761, https://doi.org/10.1130/GES02419.1.

Science Editor: Andrea Hampel
Guest Associate Editor: Karl E. Karlstrom

Received 17 February 2021
Revision received 21 May 2021
Accepted 6 July 2021

Published online 1 November 2021



# Identification of seasonal varves in the lower Pliocene Bouse Formation, lower Colorado River Valley, and implications for Colorado Plateau uplift

**Jon E. Spencer[1,*], Kurt N. Constenius[1,*], David L. Dettman[1,*], and Kenneth J. Domanik[2,*]**

[1]Department of Geosciences, The University of Arizona, 1040 E. 4th Street, Tucson, Arizona 85721, USA
[2]Lunar and Planetary Laboratory, The University of Arizona, Tucson, Arizona 85721, USA

## ABSTRACT

**The cause of Cenozoic uplift of the Colorado Plateau is one of the largest remaining problems of Cordilleran tectonics. Difficulty in discriminating between two major classes of uplift mechanisms, one related to lithosphere modification by low-angle subduction and the other related to active mantle processes following termination of subduction, is hampered by lack of evidence for the timing of uplift. The carbonate member of the Pliocene Bouse Formation in the lower Colorado River Valley southwest of the Colorado Plateau has been interpreted as estuarine, in which case its modern elevation of up to 330 m above sea level would be important evidence for late Cenozoic uplift. The carbonate member includes laminated marl and claystone interpreted previously in at least one locality as tidal, which is therefore of marine origin. We analyzed lamination mineralogy, oxygen and carbon isotopes, and thickness variations to discriminate between a tidal versus seasonal origin. Oxygen and carbon isotopic analysis of two laminated carbonate samples shows an alternating pattern of lower $\delta^{18}O$ and $\delta^{13}C$ associated with micrite and slightly higher $\delta^{18}O$ and $\delta^{13}C$ associated with siltstone, which is consistent with seasonal variation. Covariation of alternating $\delta^{18}O$ and $\delta^{13}C$ also indicates that post-depositional chemical alteration did not affect these samples. Furthermore, we did not identify any periodic thickness variations suggestive of tidal influence. We conclude that lamination characteristics indicate seasonal genesis in a lake rather than tidal genesis in an estuary and that the laminated Bouse Formation strata provide no constraints on the timing of Colorado Plateau uplift.**

## INTRODUCTION

The Colorado Plateau and eastern Mojave Desert of the American Southwest were part of cratonic North America during Paleozoic time as indicated by the thin (~1 km), largely marine Paleozoic strata that blanketed the area and that are so well exposed in the Grand Canyon (Stone et al., 1983; Sloss, 1988). Uplift of the Colorado Plateau from near sea level to modern elevations of ~2 km resulted from post-Paleozoic tectonic processes that are incompletely understood and the topic of many investigations. Uplift has been attributed to removal of all or part of the dense, underlying mantle lithosphere during Late Cretaceous and Paleogene low-angle subduction (Bird, 1988; Spencer, 1996) and hydration of mantle lithosphere or lower crust by slab-derived fluids (Humphreys et al., 2003; Jones et al., 2015; Porter et al., 2017; Levandowski et al., 2018). Uplift has also been attributed to post-subduction processes including uplift driven by the dynamic pressure of rising asthenosphere (Moucha et al., 2008, 2009), detachment and sinking of dense mantle lithosphere (van Wijk et al., 2010; Crow et al., 2011; Levander et al., 2011; Karlstrom et al., 2012; Walk et al., 2019), and heating following inflow of underlying asthenosphere (Roy et al., 2009). Uplift related to low-angle subduction would have occurred during or immediately following slab fallback or meltback as indicated by the westward sweep of mid-Cenozoic arc magmatism (e.g., Coney and Reynolds, 1977; Spencer, 1996) and by calculations of changing slab thermal and mechanical integrity during low-angle subduction (Severinghaus and Atwater, 1990; Spencer, 1994). In contrast, uplift related to post-subduction processes would be late Cenozoic and likely ongoing (e.g., Moucha et al., 2009; Karlstrom et al., 2012). As a result of these contrasting inferred uplift ages, determination of the time of Colorado Plateau uplift is critical to understanding which broad class of uplift mechanisms is primarily responsible for Plateau uplift.

The Cenozoic paleoelevation history of the Colorado Plateau has been difficult to determine despite the application of a variety of techniques over many decades (e.g., Sahagian et al., 2002; Huntington et al., 2010). The lower Pliocene Bouse Formation in the lower Colorado River Valley (Fig. 1) consists of limestone and fine-grained clastic strata that have been interpreted as estuarine and therefore were deposited below sea level (Lucchitta, 1979; Buising, 1990; Lucchitta et al., 2001; McDougall and Miranda-Martínez, 2014; O'Connell et al., 2017, 2020; Dorsey et al., 2018; Gardner and Dorsey, 2020). These strata are now exposed at elevations of up to 330 m in southern exposures and 555 m in northern exposures, which has led to the interpretation

Jon Spencer https://orcid.org/0000-0003-4464-6332
*E-mails: spencer7@email.arizona.edu; kconstenius@comcast.net; dettman@arizona.edu; domanik@lpl.arizona.edu

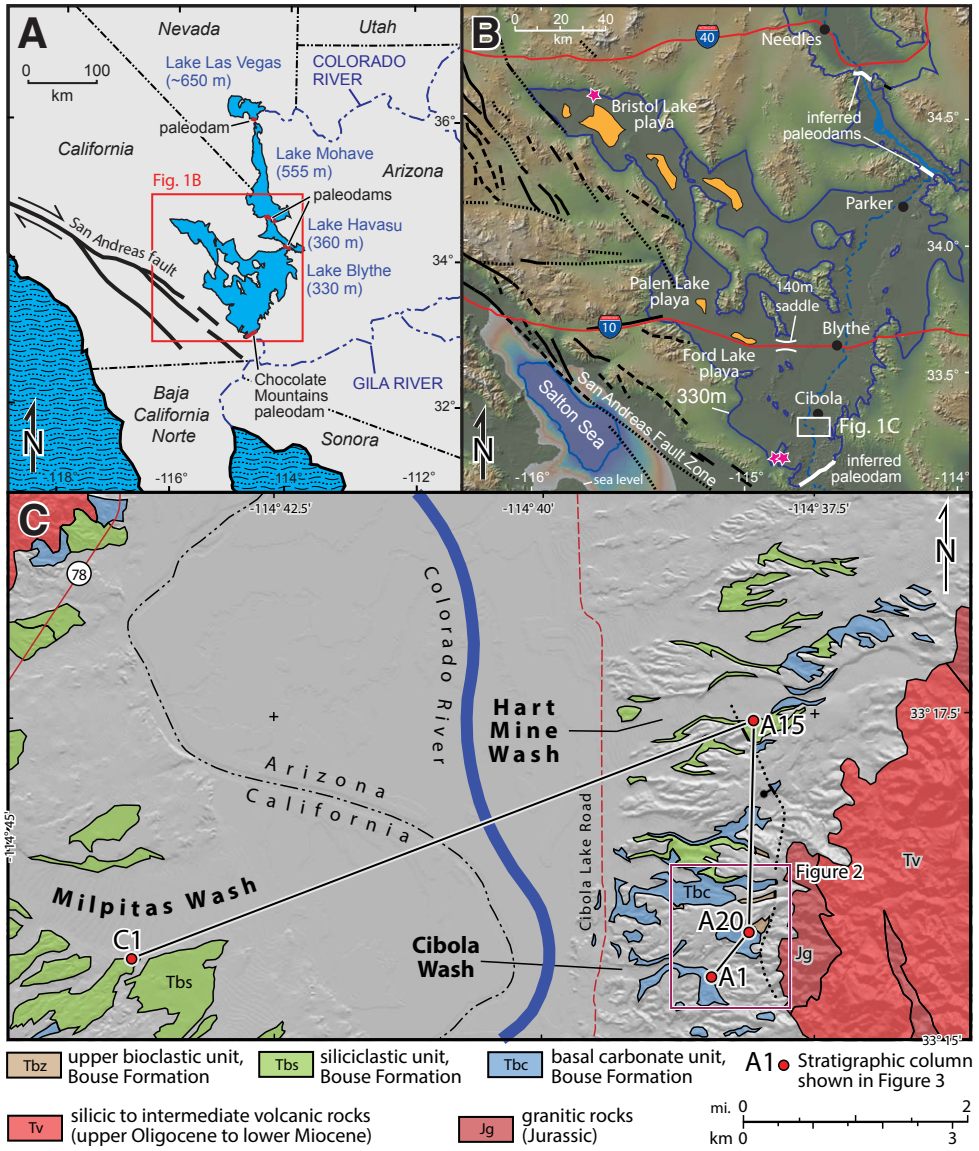


**Figure 1. (A) Map of the lower Colorado River region and adjacent areas that shows the inferred extent of the system of four lakes that resulted from first-arriving Colorado River water entering closed basins of the Basin and Range province at ca. 4.9 Ma (Spencer et al., 2008; Pearthree and House, 2014; Crow et al., 2021). (B) Greater Blythe basin, including Bristol basin, with 330-m-elevation outline showing maximum lake extent as indicated by the distribution of the basal carbonate unit of the Bouse Formation. Star symbols indicate locations of 4.83 Ma Lawlor Tuff interbedded with the Bouse Formation (Sarna-Wojcicki et al., 2011; Spencer et al., 2013; Harvey, 2014; Dorsey et al., 2018). (C) Geologic map of the Bouse Formation and local bedrock geology near the southern end of Blythe basin (modified from Gootee et al., 2016).**

that uplift of the Colorado Plateau occurred in the past 5–6 Ma and was greater closer to the plateau (Lucchitta, 1979; Lucchitta et al., 2001). In this article, we present new data from laminated Bouse marl and claystone in the basal carbonate member of the southern Bouse Formation that support lacustrine rather than estuarine deposition. This, in turn, detracts from the interpretation that the Bouse Formation is relevant to the timing of Colorado Plateau uplift.

## Bouse Formation

The lower Pliocene Bouse Formation in the lower Colorado River Valley of southeastern California, western Arizona, and southernmost Nevada (USA), consists typically of 1–20 m of bedrock-coating travertine, bedded marl, and bioclastic limestone overlain conformably by claystone, siltstone, and fine silty sandstone. These strata are in turn overlain unconformably by Colorado River sand and gravel and alluvial fan sediments (Metzger et al., 1973; Metzger and Loeltz, 1973; Buising, 1990; House et al., 2008; Pearthree and House, 2014; Homan, 2014; Gootee et al., 2016; Dorsey et al., 2018; O'Connell et al., 2017, 2020; Gardner and Dorsey, 2020). The Bouse Formation onlaps onto alluvial fan sediments and bedrock hillslopes and represents abrupt inundation of a previously subaerial environment. Blythe basin is the southernmost and largest of the basins in which the Bouse Formation was deposited (Fig. 1). The Colorado River flows through the axis of the basin where Bouse Formation has been recognized in wells of up to 280 m below sea level (Metzger et al., 1973; Cassidy et al., 2018). The axial valley may be a product of transtension in a broad, right-lateral shear zone associated with development of the San Andreas transform plate boundary during the past 10–12 Ma (Richard, 1993; Thacker et al., 2020).

Inundation leading to deposition of the Bouse Formation has been attributed to regional subsidence resulting in marine incursion during early opening of the nearby Gulf of California (Lucchitta, 1979; Buising, 1990; Lucchitta et al., 2001; McDougall and Miranda-Martínez, 2014; Dorsey et al., 2018) or

to filling of closed basins by first-arriving Colorado River water (Spencer and Patchett, 1997; House et al., 2008; Spencer et al., 2008, 2013; Pearthree and House, 2014; Crow et al., 2021). A lacustrine origin is supported by Sr, O, and C isotopic data from basal carbonates (Spencer and Patchett, 1997; Poulson and John, 2003; Roskowski et al., 2010; Bright et al., 2018a), consistent maximum elevations of Bouse deposits within proposed paleolake basins (Spencer et al., 2013; Pearthree and House, 2014), palaeoecological analysis of fossil communities in Blythe basin (Bright et al., 2018b), and sedimentological evidence of floodwater influx from northern sources immediately preceding Bouse deposition in northern Mohave Valley (House et al., 2008; Pearthree and House, 2014). A marine origin is supported by the presence of several typically marine organisms including foraminifera, barnacles, and fish that are represented by shells and fossils from low elevations in the axis of Blythe basin (Smith, 1970; Todd, 1976; Crabtree, 1989; McDougall, 2008; McDougall and Miranda-Martínez, 2014; Dorsey et al., 2018), although a variety of factors allow for the possibility that all fauna lived in a brackish lacustrine environment (Bright et al., 2018b). In addition, some sedimentological features have been interpreted to indicate a tidally influenced estuarine origin (Buising, 1990; O'Connell et al., 2017, 2020; Dorsey et al., 2018; Gardner and Dorsey, 2020).

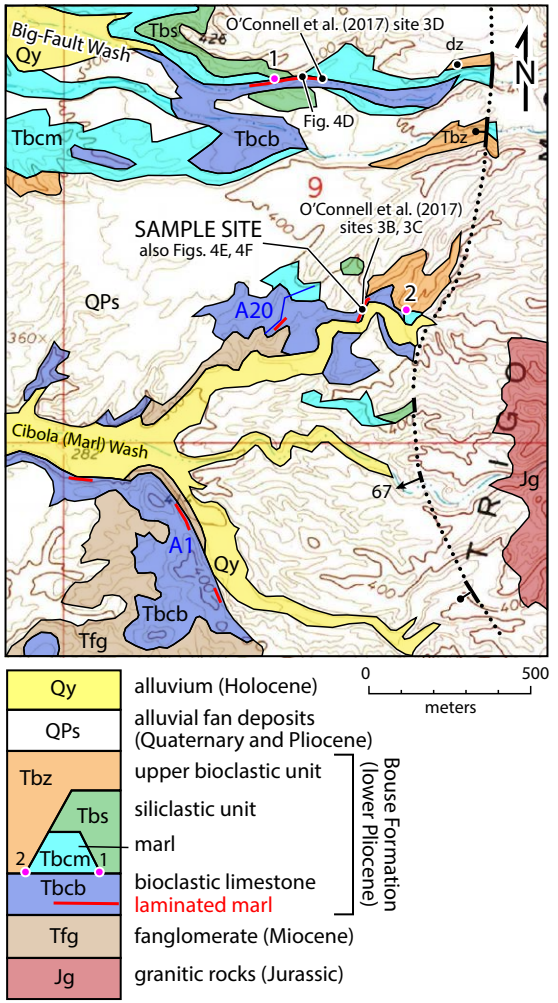


**Figure 2. Geologic map of the upper Cibola Wash area, modified from Gootee et al. (2016), shows the location of Cibola samples 20920–1UU and 20920–1L ("SAMPLE SITE"; 33.26332°N, 114.63602°W). Locations of laminated marl (red lines) correspond to Marl 1 of Homan (2014). A1 and A20 are approximate locations of measured section from Homan (2014) and are shown in Figure 3; blue line next to A20 indicates transect for the measured section. Numbers 1 and 2 indicate locations where units are missing from the stratigraphy due to erosion or extension at the head of slide masses. Laminated and cross-bedded marl sites studied by O'Connell et al. (2017) and interpreted as tidal in origin are also shown (sites 3B–3D). The distance between our Cibola Wash samples and samples 3B and 3C of O'Connell et al. (2017) is probably <2 m stratigraphically and <10 m parallel to bedding; dz indicates the location of sand sample JES-14–534, which yielded a detrital zircon age profile from 94 zircon grains that is statistically indistinguishable from three populations of ancient Colorado River sand (Spencer et al., 2015).**

In the lacustrine interpretation, deposition of the Bouse Formation resulted from the first arrival of Colorado River water and sediment to a string of closed basins in the Basin and Range province. It marks the top-down initiation of a new river and incision of the modern Grand Canyon (e.g., Spencer and Patchett, 1997; Spencer and Pearthree, 2001; House et al., 2008). In the estuarine interpretation, the Bouse Formation records a phase of subsidence associated with early rifting in the Gulf of California that is not obviously or necessarily related to Colorado River arrival (e.g., Buising, 1990; Dorsey et al., 2018; O'Connell et al., 2020; Gardner and Dorsey, 2020). Furthermore, the presence of Bouse Formation of marine or estuarine origin at significant modern elevation would indicate the approximate amount of tectonic uplift since deposition (Lucchitta, 1979; Lucchitta et al., 2001), ignoring the influence of eustatic sea-level fluctuations since the early Pliocene (Winnick and Caves, 2015; Gasson et al., 2016; Raymo et al., 2018). Proposed uplift has been tied to the timing of uplift of the Colorado Plateau and is a major reason for broad interest in the Bouse Formation.

## PURPOSE AND METHODS

The study by O'Connell et al. (2017) of the southernmost area of Bouse Formation exposures (Figs. 1–2) identified several types of sedimentological features that were interpreted as representing the activity of tides and led to the conclusion that some carbonates and related sediments in the basal carbonate unit of the Bouse Formation (Fig. 3) were deposited in an estuary or tidal flat.

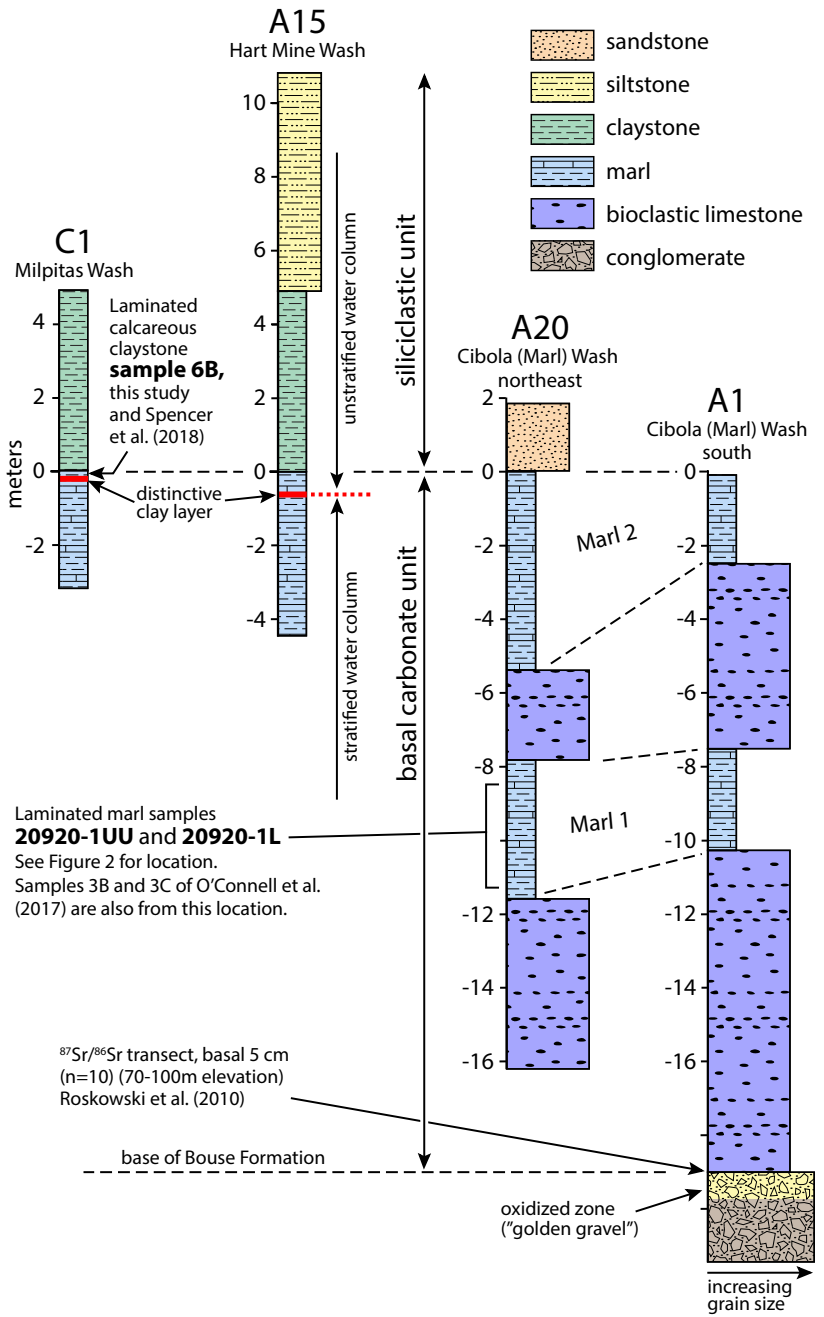


Layered sequences of laminations or thin beds that are plausibly the result of daily (diurnal) or twice daily (semidiurnal) tidal cycles were analyzed using Fourier spectral analysis to identify periodicities associated with tides. One laminated carbonate sequence from the basal carbonate unit in the Cibola area (Figs. 2–3), with 82 lamination couplets (paired light and dark layers), yielded two peaks with one that is twice the frequency of the other (fig. 3B in O'Connell et al., 2017). These were interpreted as representing superimposed diurnal and semidiurnal tidal cycles. Least squares fitting of sine waves over a range of wavelengths identified longer wavelength periodicities at 4, 5, 6, 8, 11, and 13 couplets per cycle that were interpreted as incomplete records of 14-day, spring-neap tidal cyclicity in tidal flat environments at three different sample sites in the Cibola area (O'Connell et al., 2017).

Our study was designed to test the tidal hypothesis for lamination genesis proposed by O'Connell et al. (2017) by further examining southern Bouse laminated sediments, including identification of tidal signatures from lamination thickness data. Sedimentation rates of hundreds of millimeters per year, equivalent to tens of meters per century, are implied by the tidal interpretation of laminated marl in the Cibola area. This interpretation is difficult to reconcile with a previous study (Homan, 2014) that concluded that laminations in nearby Milpitas Wash were deposited annually as varves, which implies a sedimentation rate hundreds of times slower than the rate for tidal deposition. Considering that the laminations in the two areas occur in the same basal carbonate unit of the Bouse Formation and are less than 10 km apart, it seemed likely to us that

**Figure 3. Stratigraphic columns for the Bouse Formation are shown at four sites in southern Blythe basin seen in Figure 1 (simplified from Homan, 2014). Also shown is the distinctive clay layer identified by Bright et al. (2016) at the upward transition in the hydrologic environment from an isotopically and geochemically stratified water body to a relatively homogeneous water body. Stratigraphic locations of laminated strata sampled for this study and sampled by O'Connell et al. (2017) are also shown for columns C1 and A20.**

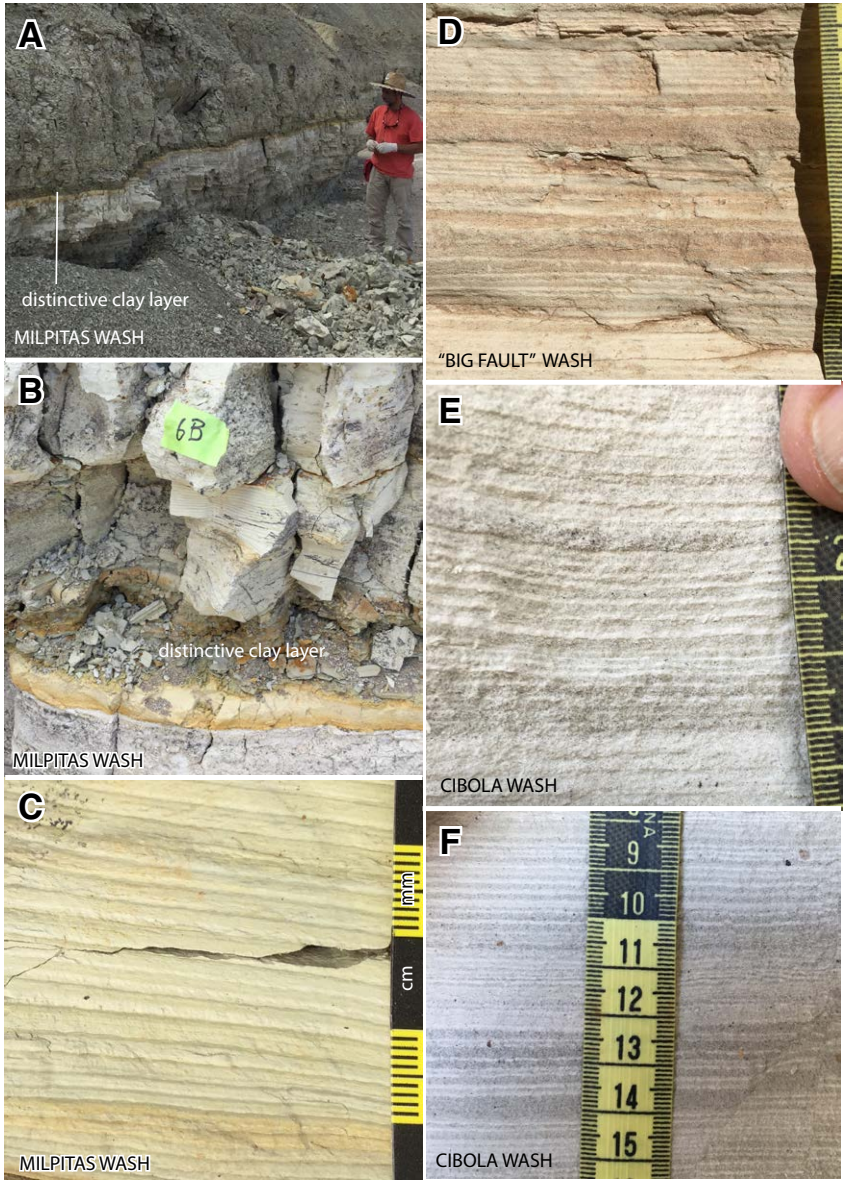


**Figure 4. Outcrop pictures show laminated marl and claystone from the basal carbonate unit of the Bouse Formation. (A, B) Location of sample 6B in Milpitas Wash (33.26044°N, 114.73059°W). (C) Laminated calcareous claystone of sample 6B in lower Milpitas Wash. (D) Laminated marl in slot canyon in Big Fault Wash (informal name) (see Figure 2 for location). Smallest scale graduations are in millimeters. (E, F) Calcareous (white) and silty (gray) laminations in upper Cibola Wash at SAMPLE SITE location seen in Figure 2.**

they were both produced by similar processes and that additional study was warranted.

We visited multiple exposures of laminated Bouse strata in the lower Milpitas Wash area in southeastern California and the Cibola area in western Arizona (Figs. 1C and 2) and collected samples from two areas where laminations are numerous, in continuous sequence of tens to hundreds of laminations, and have sharp boundaries so that thicknesses could be accurately measured. Laminated marl was sampled in lower Milpitas Wash (site "C1" in Fig. 1C), where lamination boundaries are generally sharp (Fig. 4C). Laminations at this site, located at the top of the basal carbonate unit and just below the siliciclastic unit ("sample 6B" in Figs. 3 and 4C), were interpreted as varves (Homan, 2014) deposited annually in a "quiet offshore subtidal environment" (Dorsey et al., 2018). Samples were also collected from upper Cibola Wash (an informal name, also known as "Marl Wash"; Figs. 3 and 4E–4F) at the same outcrop where evidence of tidal activity was proposed by O'Connell et al. (2017). Polished thin sections of laminated samples from both areas were scanned with a Cameca SX100 Ultra electron microprobe to produce images revealing element abundance, mineral composition, and grain angularity. Lamination thicknesses were measured from one Milpitas Wash sample and evaluated for thickness periodicity with Fourier-transform spectral-power analysis.

Two samples of laminated marl from the Cibola area were analyzed for oxygen and carbon isotope ratios. For each sample, 12 alternating white and dark laminations in continuous sequences were sampled with a microscope-mounted 0.3-mm-diameter dental-drill bur. Carbonate in each microsample was analyzed for oxygen and carbon isotopes using an automated carbonate preparation device (KIEL-III) coupled to a gas-ratio mass spectrometer (Finnigan MAT 252). Powdered samples were reacted with dehydrated phosphoric acid under vacuum at 70 °C. Phosphoric acid does not react with silicates or organic matter in samples. One sigma uncertainty of isotope measurements is ± 0.10‰ for $\delta^{18}O$ and ± 0.08‰ for $\delta^{13}C$ based on repeated measurements of NBS-19 and NBS-18. NBS-19 (n = 5) is processed with every daily batch

of samples. NBS-18 is run weekly and whenever operating conditions or focusing parameters are changed. Assigned values relative to Vienna Pee Dee Belemnite (VPDB) ($\delta^{13}C$, $\delta^{18}O$) used for these standards are +1.95‰ and –2.20‰, respectively, for NBS-19, and –5.01‰ and –23.2 ‰, respectively, for NBS-18. Sample analysis data are reported in the Supplemental Material[1]. All analyses are reported relative to the VPDB standard (Coplen, 1994).

## LAMINATION COMPOSITION

Electron-microprobe maps of total electron backscatter (BSE) and of calcium and silicon abundance in a polished thin section of laminated marl from lower Milpitas Wash show clear alternations in the ratio of calcite to clay with very few identifiable silicic grains (Figs. 5A–5C; see Appendix for methods). A sequence of BSE images at progressively greater magnification (Figs. 5D–5F) shows that calcareous laminations consist largely of 2–10 μm calcite grains. A sequence of 21 photographs of a polished thin section of this unit (Spencer et al., 2018) revealed ambiguity in assigning lamination boundaries to five of 32 laminations, including two calcareous laminations that are weakly defined and only slightly more calcareous than bounding claystone laminations.

Electron-microprobe maps of calcium, silicon, and potassium in a polished thin section of laminated marl from upper Cibola Wash show clear alternations of micrite and siltstone in which calcium is concentrated in micrite and silicon and potassium are concentrated in siliciclastic layers (Fig. 6). Magnesium, sodium, and aluminum are also associated with silty layers in electron microprobe images as is expected for siliciclastic grains. It is also apparent in the microprobe images that the sharpness of lamination transitions is variable and that some laminations have slightly irregular boundaries. Gradational boundaries for some laminations are especially apparent at higher magnification (Fig. 6, lower). At even higher magnification, ~2–20 μm calcite grains with minor clay and other minerals make up a calcareous lamination (Fig. 7A). This contrasts with the relatively coarse (40–150 μm) angular minerals in a silty lamination (Fig. 7B). The high angularity of siliceous grains, with highly elongate mica flakes, indicates minimal transport by fluvial processes, wave action, or repetitive tidal currents. Siliciclastic mineralogy suggests a granitic source, which is consistent with Jurassic granitoids exposed in the adjacent range front less than 1 km away (Fig. 1).

## OXYGEN AND CARBON ISOTOPES

Individual laminations from two laminated silty marl samples collected from the basal carbonate unit in upper Cibola Wash (Figs. 2–3) were analyzed for oxygen and carbon isotope ratios. Resulting analyses revealed alternating $\delta^{18}O$ and $\delta^{13}C$ with positive covariance in which the higher $\delta^{18}O$ and $\delta^{13}C$ are associated with silty laminations (Fig. 8). A continuous, high-resolution sequence of samples, from the center of a dark silty layer through a light calcareous layer to the overlying dark silty layer, yielded the same relationship in which isotopic variation corresponds to minor variations in color such that darker colors correspond to higher $\delta^{18}O$ and $\delta^{13}C$ (Fig. 9). Positive covariance of isotopic composition is apparent in a diagram of $\delta^{18}O$ versus $\delta^{13}C$ in which lines link adjacent laminations (Fig. 10).

Positive covariance of $\delta^{18}O$ and $\delta^{13}C$ is characteristic of lake sediments from other lacustrine settings, especially within closed basins, where the range of isotopic compositions is greater over larger stratigraphic intervals (Fig. 11; Talbot, 1990; Drummond et al., 1995). Included in Figure 11 are data on the basal 5 cm of Bouse Formation marl over a range of elevations in Cibola Wash (Roskowski et al., 2010). Also plotted are $\delta^{18}O$ and $\delta^{13}C$ from a set of laminations from Milpitas Wash (sample 6B in Figs. 3 and 4B), where only two of seven dark, silty layers yielded enough carbonate for analysis (square points in Fig. 11). All six analyses, with $\delta^{18}O$ at approximately –9‰ to –10‰, fall in a cluster slightly to the left of the stratigraphically lower, more calcareous laminations in Cibola Wash (Fig. 11). All analyses from both sites are characterized by $\delta^{18}O$ of less than –7‰ VPDB; such values are not found in unaltered marine carbonates and are extremely rare in estuarine systems (e.g., Ingram et al., 1996; Sampei et al., 2005).

## PERIODIC CHARACTERISTICS OF LAMINATION THICKNESSES

Milpitas Wash site C1 includes laminated strata with generally sharp, planar boundaries between darker claystone laminations and lighter calcareous laminations (Fig. 4C). Thickness measurements of a sequence of 69 laminations, in which each lamination consists of a couplet of lower calcareous and upper clay-rich components, identified a bimodal distribution of thicknesses with greater thicknesses above about layer 50 (Fig. 12A). There is little evidence of other trends or an overarching pattern in this data set except perhaps for slightly lower thicknesses for, approximately, layers 20–45. The simplest general interpretation is that something changed in the geologic environment at about the time of lamination 50 that resulted in thicker laminations (e.g., Cohen et al., 2006).

The 69-layer thicknesses were analyzed by Fourier spectral analysis using PAST© software (Hammer et al., 2001), which yielded a simple periodogram showing identified dominant frequencies in the thickness sequence. Only one peak, with a period of 60.4 laminations, is statistically significant in this analysis. That peak is apparent in Figure 12A, where the slight trough in the middle of the graph and the upturn at the left and, especially, the right end are reflected in a sine wave with a frequency of 60.4 layers per cycle. To evaluate the significance of the Fourier spectral analysis, we subtracted this sinusoidal component from the thickness measurements and recalculated the correlation coefficient associated with a least-squares fit to a sloping line. As shown in Figure 12B, the correlation coefficient is greater. However, only 1.14 cycles are represented by the power spectrum peak at this frequency. Consequently, it is not possible to distinguish between a truly periodic component to the thickness data and an upturn at lamination 50 that reflects a non-periodic geologic event or process.

To further evaluate the significance of periodic tidal signatures in Bouse strata, we applied Fourier

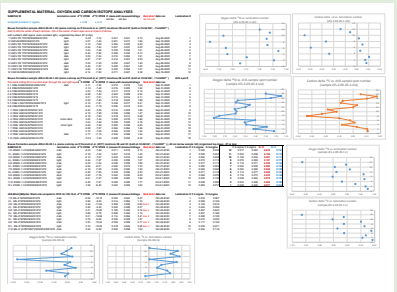

[1]Supplemental Material. Oxygen and carbon isotope analyses of laminated Bouse marl. Please visit https://doi.org/10.1130/GEOS.S.16416969 to access the supplemental material, and contact editing@geosociety.org with any questions.

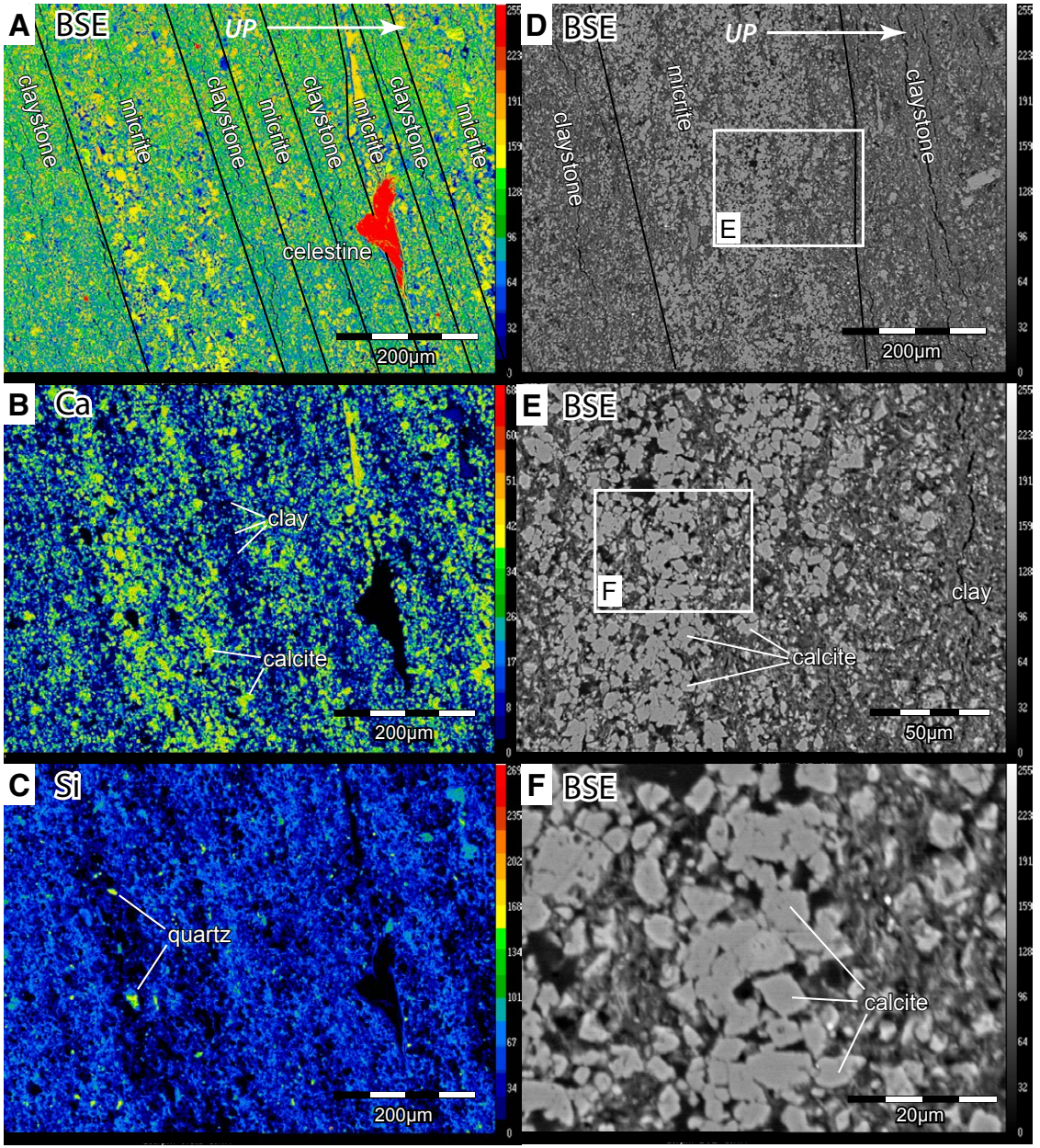


**Figure 5. Electron microprobe maps of a polished thin section of Milpitas Wash laminated claystone are shown. (A) Total electron backscatter (BSE), (B) calcium, and (C) silicon distribution and concentration show that the laminated character of the claystone results from varying ratios of clay to calcite with very little silt or sand. Warmer colors for calcium and silicon correspond to greater concentration. Warmer colors for total electron backscatter correspond to elements with more massive nuclei. Large celestine ($SrSO_4$) with three other very small grains of similar backscatter character (red color) are of unknown origin. (D, E, F) Total electron backscatter maps at progressively greater magnification indicate that marl layers contain abundant 2–10 µm calcite grains. White box in D shows area of E. White box in E shows area of F.**

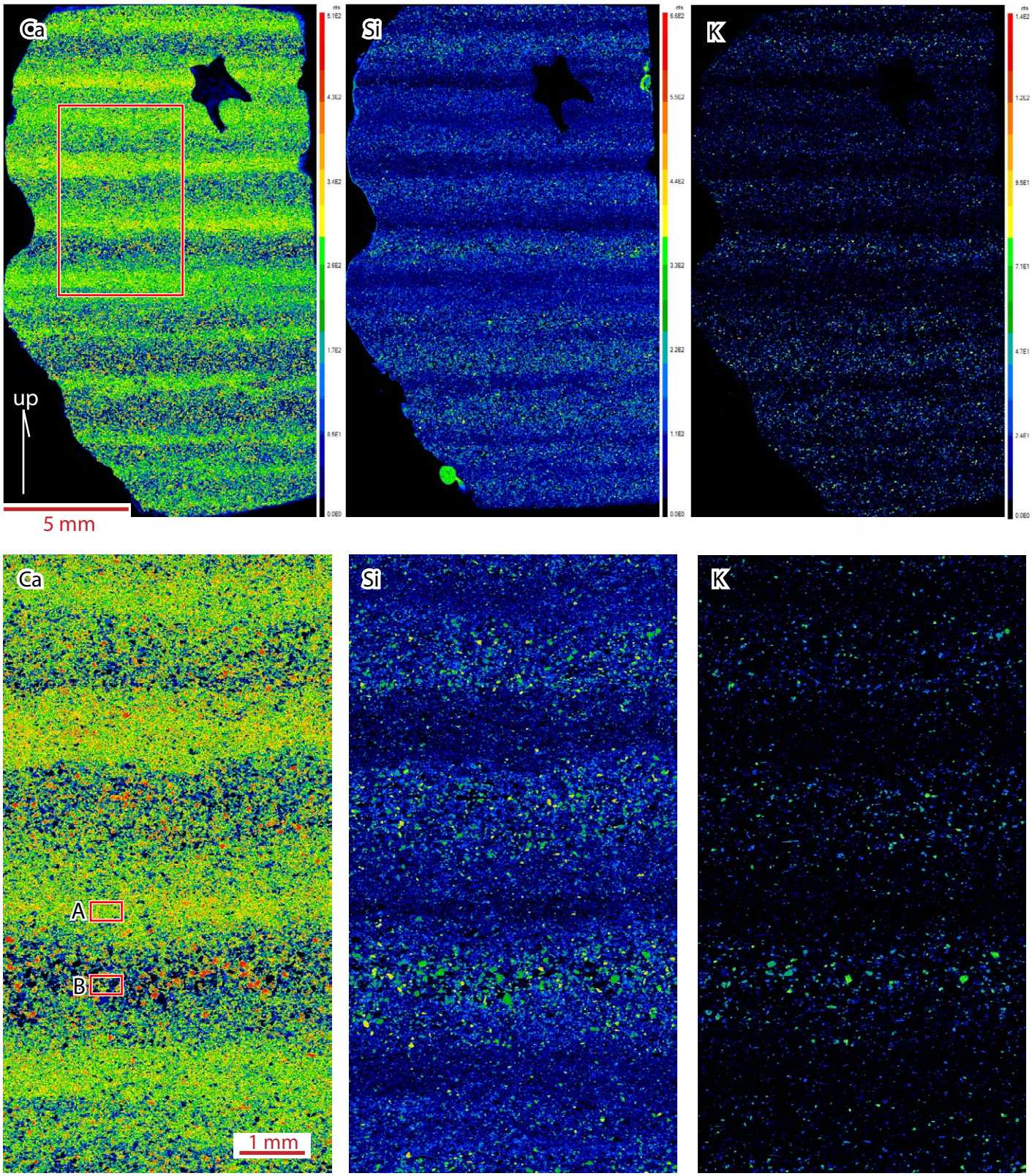


**Figure 6. Electron-microprobe maps show calcium, silicon, and potassium abundance in a polished thin section of laminated marl from upper Cibola Wash (SAMPLE SITE in Figure 2). Warmer colors correspond to greater elemental concentration. Box in upper left image shows the location of lower images with greater magnification. Boxes labeled A and B represent locations of images in Figure 7.**

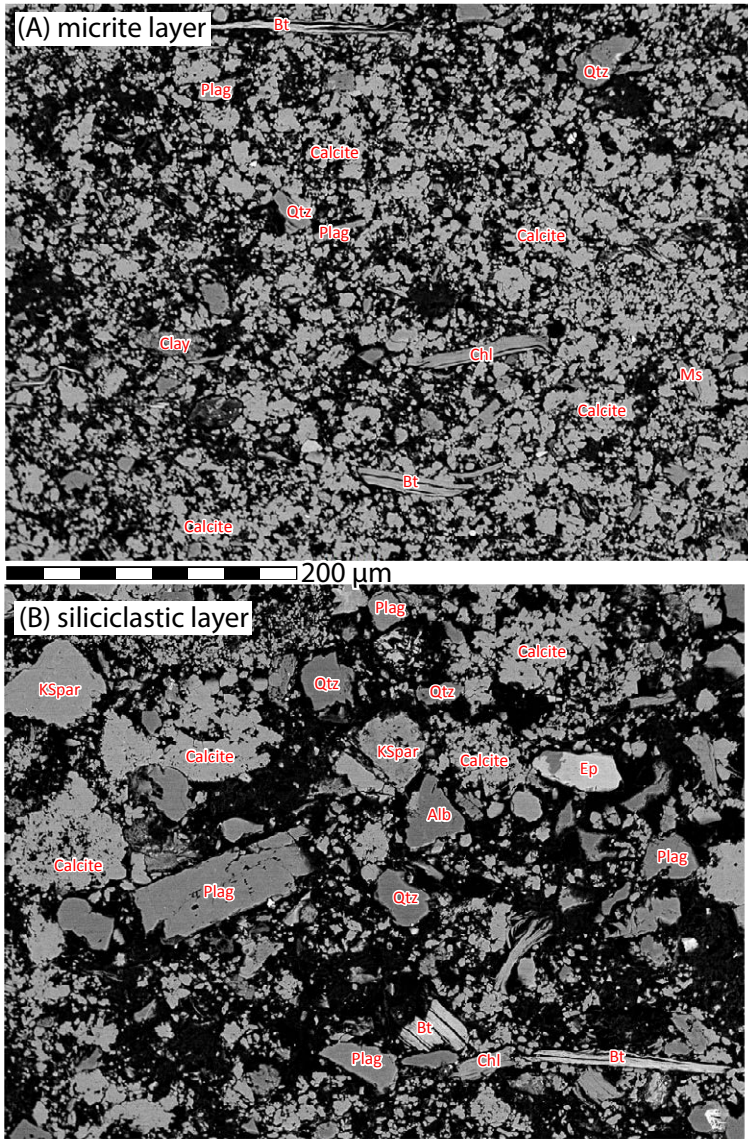


**Figure 7. Images show (A) a calcareous lamination and (B) a silty lamination. Locations are shown in Figure 6, lower left. Plag—plagioclase feldspar; Qtz—quartz; chl—chlorite; Ms—muscovite; Bt—biotite; Alb—albite; Ep—epidote. Black areas show where clay was inadvertently removed during thin section polishing. (A) The vast majority of the light-colored minerals are calcite, as indicated by calcium abundance shown in Figure 6, with less abundant, fine grains of quartz and plagioclase and flakes of mica. (B) Silty lamination with angular grains of feldspar and quartz and mica flakes of up to 150 µm in diameter.**

spectral analysis to data represented in figures 3B–3C of O'Connell et al. (2017). As with Milpitas Wash sample 6B, we combined light and dark layers (dark on top) before analysis. Fourier power-spectrum analysis of the two lamination sequences did not identify any spectral peaks with statistical confidence above the 95% level (Spencer et al., 2018). This lack of statistical significance is possibly exacerbated by a problem with the lamination thickness data reported by O'Connell et al. (2017) in which the sample 3B laminations include an exact duplication of thickness measurements for laminations 54–89 and 90–125. With Fourier spectral analysis, the null hypothesis is that all spectral power is random noise without any periodic signal that can be extracted from the complex power spectra. Failure to disprove the null hypothesis at the 95% confidence level is interpreted here to indicate that there are no statistically significant periodicities in the lamination data reported by O'Connell et al. (2017). Finally, we note that the Fourier transforms presented in figures 3B–3C of O'Connell et al. (2017) each include a peak at ~2 cycles per couplet. Since a couplet represents two thickness measurements, a peak at ~2 cycles per couplet indicates spectral power at twice the sampling frequency. Representation of frequencies higher than half the sampling frequency is inappropriate as sampled frequencies are beyond the Nyquist limit (Press et al., 1986).

## INTERPRETATION AND DISCUSSION

The composition of the marl sampled in Milpitas Wash, with alternating laminations of claystone and micrite, is consistent with an origin as annual varves reflecting seasonal changes as inferred by Homan (2014). This interpretation is based in part on the compositional contrast between the dark and light portions of each lamination as there is no plausible mechanism to trigger carbonate production on the short time frame of diurnal or semidiurnal tidal cycles. In addition, there is a complete lack of evidence for sorting of clastic material by tidal currents as there are almost no silt or sand grains or bioclastic debris. Bioclastic debris is abundant in nearshore Bouse carbonates

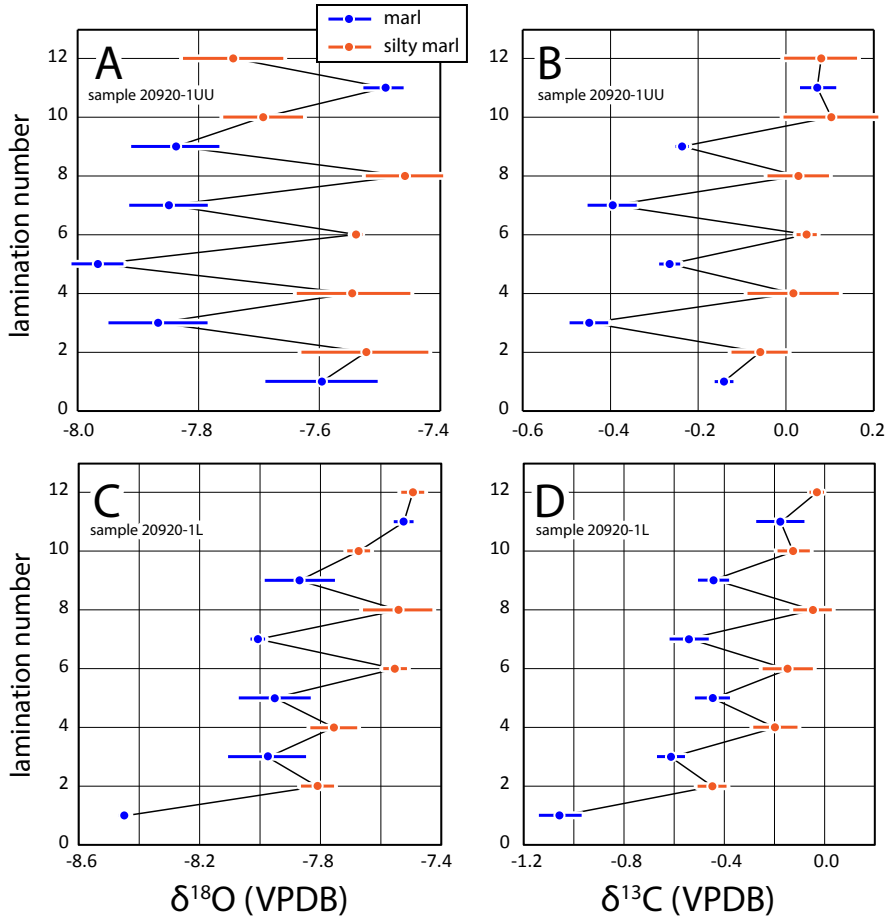


**Figure 8. Oxygen $\delta^{18}O$ and carbon $\delta^{13}C$ over 12 laminations (half couplets) in two laminated samples are shown. Both samples are from SAMPLE SITE location in Figure 2. Horizontal bars indicate 2σ analytical uncertainty. (A) $\delta^{18}O$ vs. lamination number for sample 20920–1UU. (B) $\delta^{13}C$ vs. lamination number for sample 20920–1UU. (C) $\delta^{18}O$ vs. lamination number for sample 20920–1L. (D) $\delta^{13}C$ vs. lamination number for sample 20920–1L.**

but completely absent in the Milpitas Wash sample. Lamination composition is consistent with clay and fine calcite settling out in deep water without any influence from tidal or other currents and with only seasonal variation in calcite production (e.g., Hodell et al., 1998; Teranes et al., 1999; Trapote et al., 2018). In this interpretation the 1–3 mm lamination couplets indicate a sedimentation rate of 1–3 mm/yr. In contrast, tidal rhythmite lamination couplets are deposited once or twice per day and reflect periodic sediment transport and deposition with changing grain size during each tidal cycle (e.g., Archer and Johnson, 1997; Williams, 2000; Coughenour et al., 2009). Associated deposition rates would be in the range of 0.5–2.0 m per year with currents strong enough to transport siliciclastic grains from areas submerged by high tides to sites of tidalite deposition. The almost complete lack of siliciclastic grains argues against influence from recurring tidal or shallow-water currents. Furthermore, the Milpitas Wash sample was collected from just above the distinctive clay layer that was interpreted as marking the time of maximum water depth and the initiation of lake overflow and outflow channel incision through the Chocolate Mountains to the south (Bright et al., 2016). At this time, the Milpitas Wash sample site would have been far from shore and beneath as much as 245 m of water (Fig. 13).

Laminated marl from the Cibola Wash sample site is similar to the laminated marl at the Milpitas Wash sample site but with generally less clay, more carbonate, and the addition of silt and fine sand in the darker half of the lamination couplets. We interpret the siliciclastic component as having been derived from Jurassic granitoids exposed in the mountain front directly to the east (Fig. 1C; Tosdal and Wooden, 2015) with delivery of sand and silt to the lake margin during winter storms and associated runoff. Depth could have been much shallower than at the Milpitas Wash sample site but deep enough to be unaffected by tides or other shallow water currents.

The alternation of $\delta^{18}O$ and $\delta^{13}C$ values between micritic and siliciclastic laminations in the two Cibola Wash samples is readily explained as a consequence of seasonal processes. Freshwater influx to lakes generally delivers water low in $^{18}O$ and $^{13}C$, whereas evaporation of water and dissolved $CO_2$ lead to enrichment in these heavy isotopes in remaining lake water. Preferential incorporation of $^{12}C$ into organic carbon during photosynthesis and removal through settling of organic matter, generally during times of increased sunlight and evaporation, also lead to $^{13}C$ enrichment in remaining lake water. These processes often operate together to produce positive covariation in oxygen and carbon isotopic signatures in calcareous sediments, especially in closed, semi-closed, or stratified lakes (e.g., Talbot, 1990; Drummond et al., 1995; Li and Ku, 1997). Diverse environmental situations can also affect lake water to produce negative covariance (Hodell et al., 1998; Teranes et al., 1999), but in either case covariance is a consequence of seasonal changes.

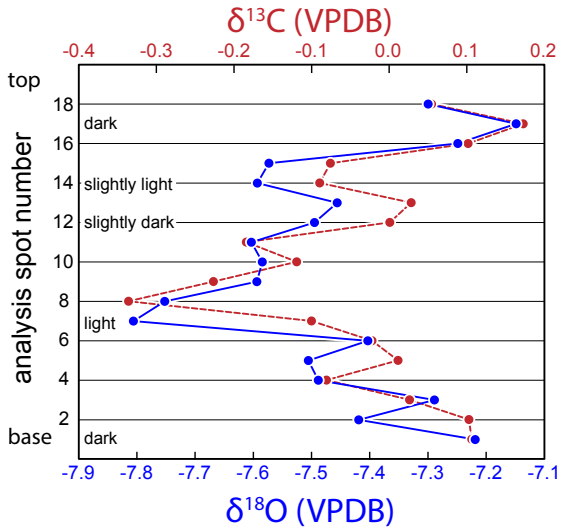


**Figure 9. Oxygen $\delta^{18}O$ and carbon $\delta^{13}C$ over three laminations drilled at two or three samples per millimeter are shown. Sampling began in the center of an underlying, dark silty lamination, continued upward through a lighter, carbonate-rich lamination, and into a dark, silty lamination. The sampled lamination is from SAMPLE SITE location in Figure 2. VPDB—Vienna Pee Dee Belemnite.**

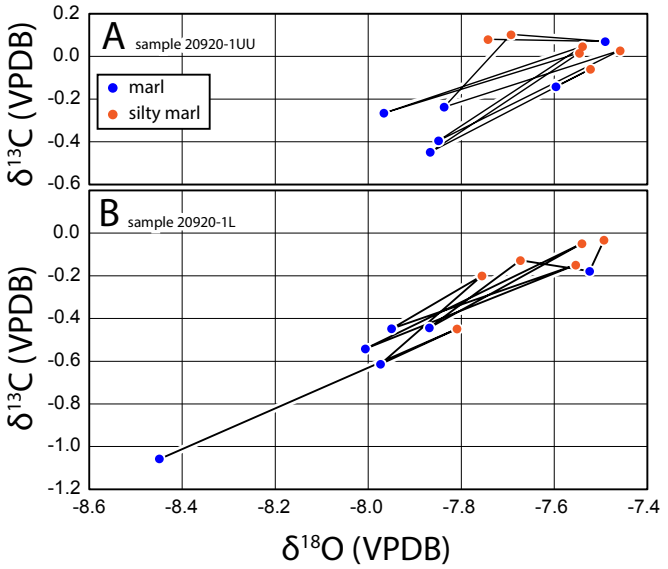


**Figure 10. Oxygen $\delta^{18}O$ versus carbon $\delta^{13}C$ over 12 laminations is shown for each of two samples from Cibola Wash; solid lines connect data points from adjacent laminations (same data are plotted in Fig. 8). (A) Sample 20920–1UU. (B) Sample 20920–1L. VPDB—Vienna Pee Dee Belemnite.**

The Colorado River drains a large upland area that receives voluminous winter precipitation and likely did so in the early Pliocene (Ibarra et al., 2018). Runoff would have been depleted in $^{18}O$ and $^{13}C$ compared to downstream lake water that had been enriched in $^{18}O$ and $^{13}C$ by in situ evaporation and precipitation of $^{12}C$-enriched organic carbon over perhaps hundreds to thousands of years. It is also possible that runoff was enriched in $^{12}C$ due to equilibration with near-surface soil carbon composed largely of $^{12}C$-enriched organic matter. Colorado River base flow derived from deeper groundwater also could have added water with higher $\delta^{18}O$ and $\delta^{13}C$ than spring and early summer runoff (Crossey et al., 2015). Our interpretation is entirely consistent with the "brackish lake–freshwater plume model for the southern Bouse Formation" of Bright et al. (2018a, p. 1902), who proposed that lower $\delta^{18}O$ values "in the micrite represent more seasonally limited epilimnic calcium carbonate production in paleolake Blythe during spring/summer floods on the early Colorado River."

Significant post-depositional alteration of just one of the two isotopes would have eliminated the isotopic covariation. We therefore interpret the isotopic data as reflecting the original composition of the carbonate rather than post-depositional alteration. Similar but negative covariation across growth bands in a Bouse barnacle shell was interpreted as evidence that carbon and oxygen isotopes are unaltered (Roskowski et al., 2010).

The Cibola Wash samples were collected from a 4-m-thick interval of laminated silty marl that is both underlain and overlain by bioclastic limestone (Fig. 3; Homan, 2014). The bioclastic limestone was deposited in nearshore environments where waves and currents produced well-sorted, sub-rounded to well-rounded calcarenite and fossil hash and a variety of types of cross beds (Gootee et al., 2016; Dorsey et al., 2018). The juxtaposition of laminated marl above bioclastic limestone in this sequence indicates increasing water depth but not so deep as to prevent seasonal delivery of silt and fine sand from the nearshore environment. Laminated marl deposition was followed by decreasing water depth and deposition of the upper bioclastic limestone layer in a nearshore environment. Overlying marl and stratigraphically

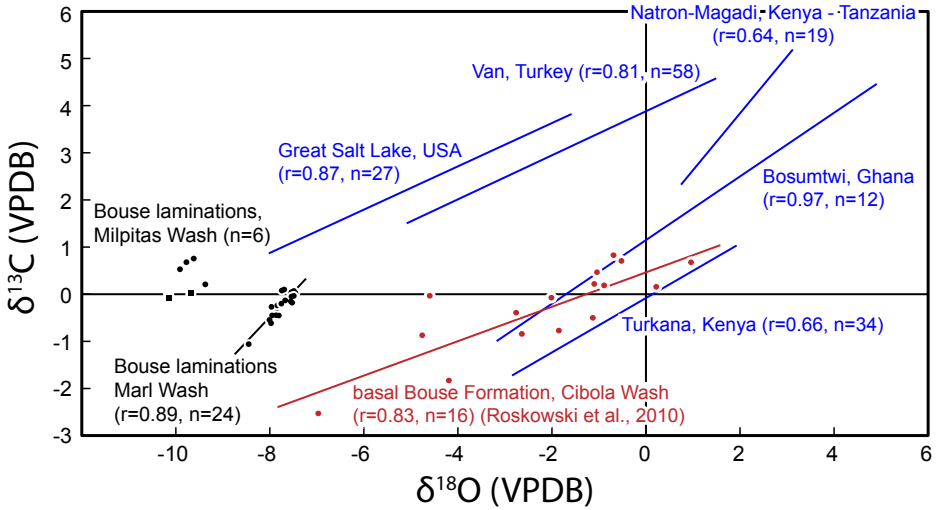


**Figure 11. Oxygen $\delta^{18}O$ versus carbon $\delta^{13}C$ is shown for lacustrine carbonates with least squares linear approximation (line), correlation coefficient (r), and number of analyses (n) for each set of analyses. Bouse lamination data presented in this study are shown in black. Calcareous Bouse strata from the basal ~5 cm of the Bouse Formation along a transect in Cibola Wash are plotted in red (from Roskowski et al., 2010). Five linear regression approximations from sediments in Quaternary lakes are plotted in blue for comparison (from Talbot, 1990; Great Salt Lake—Spencer et al., 1984, and McKenzie, 1985; Lake Van—Schoell, 1978; Natron-Magaadi lake system—Hillaire-Marcel and Casanova, 1987; Turkana—Halfman et al.,1989; Bosumtwi—Talbot and Kelts, 1986, and Talbot, 1990). VPDB—Vienna Pee Dee Belemnite.**

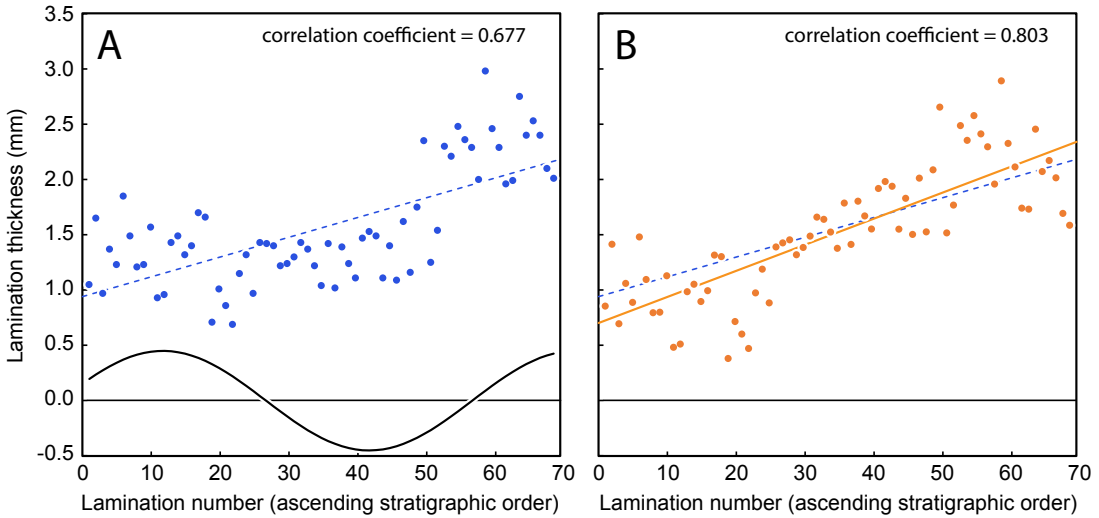


**Figure 12. (A) Lamination thickness measurements are shown from a continuous sequence of 69 calcareous claystone laminations in lower Milpitas Wash (site C1) from the basal carbonate unit just above the distinctive clay layer (see Fig. 3 for stratigraphic position and Fig. 4C for image; data from Spencer et al., 2018). Also plotted is a least-squares linear fit with a correlation coefficient of 0.677 (dashed line). Fourier spectral analysis of the plotted data identified a dominant cyclicity at 60.4 laminations per cycle (Spencer et al., 2018). A sinusoidal signal representing this cyclicity is shown below the plotted data. The amplitude and phase shift for this sinusoid were evaluated iteratively in a Microsoft Excel® spreadsheet to find the maximum correlation coefficient following subtraction. The sinusoid shown in part A is the one that maximizes the correlation coefficient as shown in part B (amplitude = 0.45 mm and phase shift = 0.055 * 2π radians where positive corresponds to shifting the sine wave to the left). (B) Lamination thicknesses are modified from part A. The value of the sinusoid at each lamination, as shown in part A, was subtracted from the data to produce a modified data set plotted in part B.**

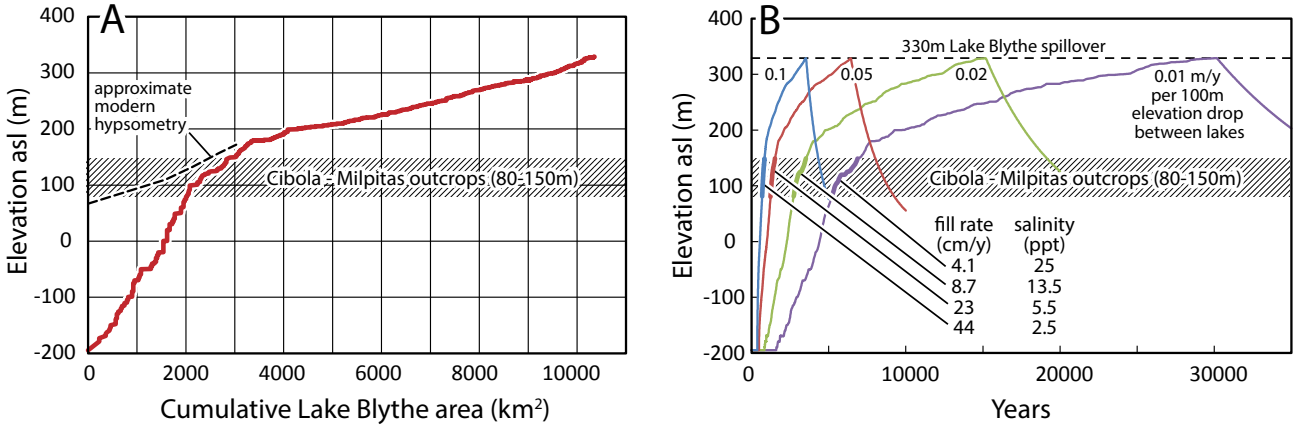


**Figure 13. (A) Hypsometric representation shows Paleolake Blythe bathymetry before deposition of the Bouse Formation and overlying strata (red line). The plotted curve was derived from a digital elevation model made by subtracting the depth to the base of the Bouse Formation, as determined by well logs, from modern elevation and then extrapolating depth contours (Spencer et al., 2008, 2013). (B) Numerical modeling of Colorado River influx to a chain of basins, with a sequence of basin fill and spill events, incision of outflow channels, and eventual draining of lakes, was used to calculate the rise and fall of Paleolake Blythe for four different incision rates (model details and parameters in Spencer et al., 2008 [see appendix], 2013). Numbers associated with each curve in the upper part of the graph indicate the model incision rate, which is higher for greater elevation drop between lakes. The fill rate and salinity are listed for each lake level curve where lake level passes upward through the elevation range of Bouse exposures in the Cibola and Milpitas Wash areas. With greater incision rates, the entire system is flushed out faster and salinities are lower. Evaluation of the ecological and salinity requirements of the Paleolake Blythe fossil community suggests salinity of 5–10 ppt (parts per thousand; Bright et al., 2018b), which is considerably less than seawater at ~35 ppt. If modern Colorado River volume and salinity, and evaporation rates in the eastern Mojave Desert, are similar to those during Bouse time, subaqueous conditions would have persisted in the Cibola-Milpitas area for ~5–15 k.y. (red and green curves).**

higher claystone and siltstone indicate return of the deep-water environment (Bright et al., 2016).

The cause of inferred shallowing associated with the upper bioclastic limestone subunit in upper Cibola Wash is uncertain. Numerical modeling of filling and spilling in a sequence of Bouse lakes indicates lake water rise followed by spillover and rapid decline with inflow and outflow channel incision rate as the primary variable controlling lake level and salinity evolution (Fig. 13; Spencer et al., 2008, 2013). Measured sections indicate substantial stratigraphic diversity for the basal carbonate unit in the Cibola area such that most stratigraphic sections do not have distinctive lower and upper bioclastic limestone subunits (Homan, 2014), which raises the possibility that shallowing leading to deposition of the upper bioclastic limestone subunit in upper Cibola Wash was a minor event. One possibility is that a brief lake lowering occurred when rising Paleolake Blythe spilled over the saddle between the lower Colorado River Valley and the basin containing Ford Lake and Palen Lake playas west of Blythe (Fig. 1B). With modern topography, this would result in only 1–2 m of water level decline, but the basin containing Ford Lake and Palen Lake playas was likely substantially deeper at 4.8 Ma and perhaps accommodated a spillover that caused an abrupt decline in lake level of 3–6 m or more. The saddle, now at 140 m elevation, is higher than the Cibola sample site at 122 m, but the saddle would have been lower before alluvial fan aggradation, and the Cibola site would have been higher prior to downfaulting on the nearby normal fault directly to the east. Maximum offset of the Bouse Formation along this pre-Quaternary, west-side-down fault is ~30 m with offset decreasing to the north over 5 km of intermittent exposure (Figs. 1C and 2; Gootee et al., 2016).

Fourier spectral analysis of 69 lamination thickness measurements from Milpitas Wash identified a statistically significant periodicity of 60.4 laminations per cycle. Lamination thicknesses plot in a horizontal band with the primary deviation represented by an abrupt increase in lamination thicknesses at about lamination 50. This deviation appears to be the primary cause of the identified periodicity. Subtracting the periodic signal from the thickness data yields a more linear trend with a higher correlation coefficient, which supports the interpretation that a periodic signal is superimposed on the linear trend. Lack of data over multiple cycles, however, renders the interpretation of a periodic tidal signature suspect. Non-periodic geologic processes could have influenced or caused the abrupt increase in lamination thicknesses without any periodic influence. The step in the data is clearly not random noise, as is apparent both from visual inspection and Fourier spectral analysis, but Fourier analysis has not demonstrated that it is periodic. This should serve as a caution about

identifying periodicity in any Fourier power spectrum without determining the number of cycles represented by power spectrum peaks.

## CONCLUSIONS

(1) Laminated marl in Milpitas Wash consists of alternating layers of claystone and micrite in which almost all calcite grains are less than ~10 μm in diameter. Internal compositional variation in each lamination is due primarily or exclusively to varying abundance of fine calcite grains. There is no evidence of sorting by grain size as is expected for transport and deposition by tidal or other nearshore or shallow water currents. We infer that the Milpitas Wash laminated strata were gently and gradually deposited in deep water on a seasonal rather than tidal schedule, which is consistent with the interpretation of Homan (2014).

(2) Laminated marl in upper Cibola Wash at the site of purported tidalites (O'Connell et al., 2017) is similar in composition and thickness to laminations at Milpitas Wash except that carbonate content is greater in the micrite layers, and texturally immature silt and fine sand are a component of the siliceous layers. Siliciclastic grains consist primarily of angular quartz and feldspar and elongate mica flakes that were not significantly rounded during transport. Granitoids exposed in the range front <1 km to the east are the obvious source of the angular grains. We infer that the siliciclastic component was derived from this range front and deposited in water that was deep enough to be unaffected by shoreline waves and currents but not so deep as to be out of reach of silt and fine sand delivered to the lake margin by winter-storm runoff.

(3) Oxygen isotope and carbon isotope analyses of carbonate from 12 laminations in each of two Cibola Wash samples indicate alternating $\delta^{18}O$ and $\delta^{13}C$ between silty and calcareous laminations. We interpret this alternating pattern to reflect seasonal variations in a lake rather than estuarine tidal ebb and flow on a daily or twice daily schedule. Specifically, runoff from the upper Colorado River basin produced a shallow, freshwater plume each spring and early summer, and carbonate produced by shallow water biological activity during these seasons reflects the low $\delta^{18}O$ and $\delta^{13}C$ of the runoff. In contrast, older, more evaporatively modified lake water with higher $\delta^{18}O$ and $\delta^{13}C$ influenced the composition of less abundant carbonates deposited during fall and winter along with fine sand that was transported by local runoff during winter storms. This interpretation is consistent with the concept of an isotopically stratified water column identified by Bright et al. (2018a) based on oxygen and carbon isotopic analysis of carbonates and ostracods with lake water stratification maintained by seasonal influx of low-$\delta^{18}O$ and low-$\delta^{13}C$ runoff from the upper Colorado River catchment.

(4) Variation of $\delta^{18}O$ and $\delta^{13}C$ in carbonate both between and within Bouse laminations reflects the absence of post-depositional alteration as these fine-scale variations would have been homogenized if significant alteration had occurred. We conclude that post-depositional alteration was minimal or non-existent as have earlier studies of $\delta^{18}O$ and $\delta^{13}C$ in barnacle-shell growth bands (Roskowski et al., 2010) and $^{87}Sr/^{86}Sr$ in Bouse carbonates and post-depositional carbonate veins, crusts, and caliches (Spencer and Patchett, 1997).

(5) Fourier spectral analysis of a sequence of 69 lamination thicknesses from a sample of Milpitas Wash calcareous claystone identified a periodicity at 60.4 laminations per cycle that could be distinguished from random noise with more than 95% confidence. However, a step in thickness data at about lamination 50 likely has a geologic origin that is not random, but it is not necessarily periodic. We conclude that inference of a periodic signal in a lamination-thickness sequence is unwarranted unless multiple cycles have actually been sampled.

(6) Spectral analysis of two lamination thickness data sets from Cibola Wash, measured by O'Connell et al. (2017) and interpreted as indicators of tidal activity, did not identify any statistically significant periodicities (Spencer et al., 2018), and one of the two data sets contains a data duplication that appears to be erroneous. Furthermore, Fourier spectral analysis by O'Connell et al. (2017) inappropriately identified periodicities higher than half of the sampling rate (Press et al., 1986).

(7) The high sedimentation rates required by the tidal interpretation of laminations in upper Cibola Wash, and the extreme contrast with annual deposition of laminations in Milpitas Wash, are unnecessary in our analysis, which indicates similar, 1–3 mm/yr sedimentation rates in both areas.

(8) We conclude that lamination thicknesses, petrology, and O and C isotopic character in the Milpitas Wash and Cibola Wash sites support seasonally varying deposition in a lacustrine environment without any influence from tides. This is consistent with the concept that the Bouse Formation is irrelevant to the timing of Colorado Plateau uplift.

### ACKNOWLEDGMENTS

We thank Andy Cohen and Jordan Bright for comments on an earlier draft that led to significant improvements, and Daniel Ibarra, David Miller, an anonymous reviewer, and associate editor Karl Karlstrom for constructive reviews that led to greater clarity and better focus. Thanks! J. Spencer thanks Jon Patchett, Phil Pearthree, Brian Gootee, and Kyle House for informative discussions over many years regarding the Bouse Formation. Geologic mapping by J. Spencer in the Cibola 7.5′ Quadrangle in 2015 was jointly funded by the Arizona Geological Survey and the U.S. Geological Survey under STATEMAP assistance award #G13AC00374.

### APPENDIX. ELECTRON MICROPROBE METHODS

Backscattered electron (BSE) imaging and chemical element X-ray mapping were performed using the CAMECA SX100 Ultra electron microprobe at the University of Arizona, equipped with an LaB6 filament electron source and five wavelength dispersive spectrometers for detecting X-rays emitted from the sample. BSE images were obtained by either scanning the electron beam over an area of the sample or, for larger areas, by moving the

sample back and forth under a stationary electron beam and recording the spatial location and number of high-energy "backscattered" electrons produced by the sample. The number of backscattered electrons scattered by the sample (and thus the brightness of the BSE image) increases with the average atomic number of the material in the sample. An image is thereby produced showing areas that differ in average atomic number, which is often useful in distinguishing different mineral species.

Chemical X-ray maps were produced by setting each spectrometer to detect the appropriate X-ray wavelength for a specified element. The sample was then moved back and forth under a stationary electron beam, and the number of X-rays produced at each point in the sample area was recorded. The number of characteristic elemental X-rays produced at any location (and thus the brightness of the X-ray image) is directly proportional to the concentration of that element at that location. As a result, the X-ray map displays the spatial variation in the chemical concentration of that element within the sample area. This technique is useful in revealing minerals with similar chemical compositions as well as chemical gradients both within individual minerals and across larger areas.

## REFERENCES CITED


Archer, A.W., and Johnson, T.W., 1997, Modeling of cyclic tidal rhythmites (Carboniferous of Indiana and Kansas, Precambrian of Utah, USA) as a basis for reconstruction of intertidal positioning and paleotidal regimes: Sedimentology, v. 44, p. 991–1010, https://doi.org/10.1111/j.1365-3091.1997.tb02174.x.

Bird, P., 1988, Formation of the Rocky Mountains, western United States: A continuum computer model: Science, v. 239, p. 1501–1507, https://doi.org/10.1126/science.239.4847.1501.

Bright, J., Cohen, A.S., Dettman, D.L., Pearthree, P.A., Dorsey, R.J., and Homan, M.B., 2016, Did a catastrophic lake spillover integrate the late Miocene early Pliocene Colorado River and the Gulf of California?: Microfaunal and stable isotope evidence from Blythe Basin, California–Arizona, USA: PALAIOS, v. 31, p. 81–91, https://doi.org/10.2110/palo.2015.035.

Bright, J., Cohen, A.S., Dettman, D.L., and Pearthree, P.A., 2018a, Freshwater plumes and brackish lakes: Integrated microfossil and O-C-Sr isotopic evidence from the late Miocene and early Pliocene Bouse Formation (California-Arizona) supports a lake overflow model for the integration of the lower Colorado River corridor: Geosphere, v. 14, p. 1875–1911, https://doi.org/10.1130/GES01610.1.

Bright, J., Cohen, A.S., and Starratt, S.W., 2018b, Distinguishing brackish lacustrine from brackish marine deposits in the stratigraphic record: A case study from the late Miocene and early Pliocene Bouse Formation, Arizona and California, USA: Earth-Science Reviews, v. 185, p. 974–1003, https://doi.org/10.1016/j.earscirev.2018.08.011.

Buising, A.V., 1990, The Bouse Formation and bracketing units, southeastern California and western Arizona: Implications for the evolution of the proto-Gulf of California and the lower Colorado River: Journal of Geophysical Research: Solid Earth, v. 95, p. 20,111–20,132, https://doi.org/10.1029/JB095iB12p20111.

Cassidy, C.E., Beard, L.S., Crow, R., Cohen, A.S., House, P.K., Pearthree, P.A., Thacker, J., and Howard, K., 2018, Subsurface data in the lower Colorado River corridor and its implications for tectonic models of basin evolution within the Palo Verde and Parker Valleys: Geological Society of America Abstracts with Programs, v. 50, no. 5, https://doi.org/10.1130/abs/2018RM-314097.

Cohen, A.S., Lezzar, K.E., Cole, J., Dettman, D., Ellis, G.S., Gonneea, M.E., Plisnier, P.-D., Langenberg, V., Blaauw, M., and Zilifi, D., 2006, Late Holocene linkages between decade–century scale climate variability and productivity at Lake Tanganyika, Africa: Journal of Paleolimnology, v. 36, p. 189–209, https://doi.org/10.1007/s10933-006-9004-y.

Coney, P.J., and Reynolds, S.J., 1977, Cordilleran Benioff zones: Nature, v. 270, p. 403–406, https://doi.org/10.1038/270403a0.

Coplen, T.B., 1994, Reporting of stable hydrogen, carbon, and oxygen isotopic abundances: Pure and Applied Chemistry, v. 66, p. 273–276, https://doi.org/10.1351/pac199466020273.

Coughenour, C.L., Archer, A.W., and Lacovera, K.J., 2009, Tides, tidalites, and secular changes in the Earth-Moon system: Earth-Science Reviews, v. 97, p. 59–79, https://doi.org/10.1016/j.earscirev.2009.09.002.

Crabtree, C.B., 1989, A new silverside of the genus *Colpichthys* (Atheriniformes: Atherinidae) from the Gulf of California, Mexico: Copeia, v. 1989, p. 558–568, https://doi.org/10.2307/1445481.

Crossey, L.C., Karlstrom, K.E., Dorsey, R., Pearce, J., Wan, E., Beard, L.S., Asmerom, Y., Polyak, V., Crow, R.S., Cohen, A., Bright, J., and Pecha, M.E., 2015, Importance of groundwater in propagating downward integration of the 6–5 Ma Colorado River system: Geochemistry of springs, travertines, and lacustrine carbonates of the Grand Canyon region over the past 12 Ma: Geosphere, v. 11, p. 660–682, https://doi.org/10.1130/GES01073.1.

Crow, R., Karlstrom, K., Asmerom, Y., Schmandt, B., Polyak, V., and DuFrane, S.A., 2011, Shrinking of the Colorado Plateau via lithospheric mantle erosion: Evidence from Nd and Sr isotopes and geochronology of Neogene basalts: Geology, v. 39, p. 27–30, https://doi.org/10.1130/G31611.1.

Crow, R.S., Schwing, J., Karlstrom, K.E., Heizler, M., Pearthree, P.A., House, P.K., Dulin, S., Jänecke, S.U., Stelten, M., and Crossey, L.J., 2021, Redefining the age of the lower Colorado River, southwestern United States: Geology, v. 49, p. 635–640, https://doi.org/10.1130/G48080.1.

Dorsey, R.J., O'Connell, B., McDougall, K., and Homan, M.B., 2018, Punctuated sediment discharge during early Pliocene birth of the Colorado River: Evidence from regional stratigraphy, sedimentology, and paleontology: Sedimentary Geology, v. 363, p. 1–33, https://doi.org/10.1016/j.sedgeo.2017.09.018.

Drummond, C.N., Patterson, W.P., and Walker, J.C.G., 1995, Climatic forcing of carbon-oxygen isotopic covariance in temperate-region marl lakes: Geology, v. 23, p. 1031–1034, https://doi.org/10.1130/0091-7613(1995)023<1031:CFOCOI>2.3.CO;2.

Gardner, K.K., and Dorsey, R.J., 2020, Mixed carbonate-siliciclastic sedimentation at the margin of a late Miocene tidal strait, lower Colorado River Valley, south-western USA: Sedimentology, v. 68, p. 1893–1922, https://doi.org/10.1111/sed.12834.

Gasson, E., DeConto, R.M., and Pollard, D., 2016, Modeling the oxygen isotope composition of the Antarctic ice sheet and its significance to Pliocene sea level: Geology, v. 44, p. 827–830, https://doi.org/10.1130/G38104.1.

Gootee, B.F., Pearthree, P.A., House, P.K., Youberg, A., Spencer, J.E., and O'Connell, B., 2016, Geologic map of the Cibola area, La Paz County, Arizona, and Imperial County, California: Arizona Geological Survey Digital Map DGM-112, scale 1:24,000, 1 plate, 21 p.

Halfman, J.D., Johnson, T.C., Showers, W.J., and Lister, G.S., 1989, Authigenic low-Mg calcite in Lake Turkana, Kenya: Journal of African Earth Sciences, v. 8, p. 533–540, https://doi.org/10.1016/S0899-5362(89)80043-0.

Hammer, Ø., Harper, D.A.T., and Ryan, P.D., 2001, PAST: Paleontological statistics software package for education and data analysis: Palaeontologia Electronica, v. 4, palaeo-electronica.org/2001_1/past/issue1_01.htm.

Harvey, J.C., 2014, Zircon age and oxygen isotopic correlations between Bouse Formation tephra and the Lawlor Tuff: Geosphere, v. 10, p. 221–232, https://doi.org/10.1130/GES00904.1.

Hillaire-Marcel, C., and Casanova, J., 1987, Isotopic hydrology and paleohydrology of the Magadi (Kenya)-Natron (Tanzania) basin during the Late Quaternary: Palaeogeography, Palaeoclimatology, Palaeoecology, v. 58, p. 155–181, https://doi.org/10.1016/0031-0182(87)90058-7.

Hodell, D.A., Schelske, C.L., Fahnenstiel, G.L., and Robbins, L.L., 1998, Biologically induced calcite and its isotopic composition in Lake Ontario: Limnology and Oceanography, v. 43, no. 2, p. 187–199, https://doi.org/10.4319/lo.1998.43.2.0187.

Homan, M.B., 2014, Sedimentology and stratigraphy of the Miocene-Pliocene Bouse Formation near Cibola, Arizona and Milpitas Wash, California: Implications for the early evolution of the Colorado River [M.S. thesis]: Eugene, Oregon, University of Oregon, 116 p.

House, P.K., Pearthree, P.A., and Perkins, M.E., 2008, Stratigraphic evidence for the role of lake spillover in the inception of the lower Colorado River in southern Nevada and western Arizona, *in* Reheis, M.C., Hershler, R., and Miller, D.M., eds., Late Cenozoic Drainage History of the Southwestern Great Basin and Lower Colorado River Region: Geologic and Biotic Perspectives: Geological Society of America Special Paper 439, p. 335–353, https://doi.org/10.1130/2008.2439(15).

Humphreys, E., Hessler, E., Dueker, K., Farmer, G.L., Erslev, E., and Atwater, T., 2003, How Laramide-age hydration of North American lithosphere by the Farallon slab controlled subsequent activity in the western United States: International Geology Review, v. 45, p. 575–595, https://doi.org/10.2747/0020-6814.45.7.575.

Huntington, K.W., Wernicke, B.P., and Eiler, J.M., 2010, Influence of climate change and uplift on Colorado Plateau paleotemperatures from carbonate clumped isotope thermometry: Tectonics, v. 29, no. TC3005, https://doi.org/10.1029/2009TC002449.

Ibarra, D.E., Oster, J.L., Winnick, M.J., Rugenstein, J.K.C., Byrne, M.P., and Chamberlain, C.P., 2018, Warm and cold wet states in the western United States during the Pliocene–Pleistocene: Geology, v. 46, p. 355–358, https://doi.org/10.1130/G39962.1.

Ingram, B.L., Conrad, M.E., and Ingle, J.C., 1996, Stable isotope and salinity systematics in estuarine waters and carbonates: San Francisco Bay: Geochimica et Cosmochimica Acta, v. 60, p. 455–467, https://doi.org/10.1016/0016-7037(95)00398-3.

Jones, C.H., Mahan, K.H., Butcher, L.A., Levandowski, W.B., and Farmer, G.L., 2015, Continental uplift through crustal hydration: Geology, v. 43, p. 355–358, https://doi.org/10.1130/G36509.1.

Karlstrom, K.E., Coblentz, D., Dueker, K., Ouimet, W., Kirby, E., Van Wijk, J., Schmandt, B., Kelley, S., Lazear, G., Crossey, L.J., Crow, R., Aslan, A., Darling, A., Aster, R., MacCarthy, J.,

Hansen, S.M., Stachnik, J., Stockli, D.F., Garcia, R.V., Hoffman, M., McKeon, R., Feldman, J., Heizler, M., Donahue, M.S., and the CREST Working Group, 2012, Mantle-driven dynamic uplift of the Rocky Mountains and Colorado Plateau and its surface response: Toward a unified hypothesis: Lithosphere, v. 4, p. 3–22, https://doi.org/10.1130/L150.1.

Levander, A., Schmandt, B., Miller, M.S., Liu, K., Karlstrom, K.E., Crow, R.S., Lee, C.-T.A., and Humphreys, E.D., 2011, Continuing Colorado plateau uplift by delamination style convective lithospheric downwelling: Nature, v. 472, p. 461–465, https://doi.org/10.1038/nature10001.

Levandowski, W., Jones, C.H., Butcher, L.A., and Mahan, K.H., 2018, Lithospheric density models reveal evidence for Cenozoic uplift of the Colorado Plateau and Great Plains by lower-crustal hydration: Geosphere, v. 14, p. 1150–1164, https://doi.org/10.1130/GES01619.1.

Li, H.-C., and Ku, T.-L., 1997, $\delta^{13}C$-$\delta^{18}O$ covariance as a paleohydrological indicator for closed-basin lakes: Palaeogeography, Palaeoclimatology, Palaeoecology, v. 133, p. 69–80, https://doi.org/10.1016/S0031-0182(96)00153-8.

Lucchitta, I., 1979, Late Cenozoic uplift of the southwestern Colorado Plateau and adjacent lower Colorado River region: Tectonophysics, v. 61, p. 63–95, https://doi.org/10.1016/0040-1951(79)90292-0.

Lucchitta, I., McDougall, K., Metzger, D.G., Morgan, P., Smith, G.R., and Chernoff, B., 2001, The Bouse Formation and post-Miocene uplift of the Colorado Plateau, *in* Young, R.A., and Spamer, E.E., eds., The Colorado River: Origin and Evolution: Grand Canyon, Arizona, USA, Grand Canyon Association Monograph 12, p. 173–178.

McDougall, K., 2008, Late Neogene marine incursions and the ancestral Gulf of California, *in* Reheis, M.C., Hershler, R., and Miller, D.M., eds., Late Cenozoic Drainage History of the Southwestern Great Basin and Lower Colorado River Region: Geologic and Biotic Perspectives: Geological Society of America Special Paper 439, p. 355–373, https://doi.org/10.1130/2008.2439(16).

McDougall, K., and Miranda-Martínez, A.Y., 2014, Evidence for a marine incursion along the lower Colorado River corridor: Geosphere, v. 10, p. 842–869, https://doi.org/10.1130/GES00975.1.

McKenzie, J.A., 1985, Carbon isotopes and productivity in the lacustrine and marine environment, *in* Stumm, W., ed., Chemical Processes in Lakes: New York, Wiley, p. 99–118.

Metzger, D.G., and Loeltz, O.J., 1973, Geohydrology of the Needles area, Arizona, California, and Nevada: U.S. Geological Survey Professional Paper 486-J, 54 p., https://doi.org/10.3133/pp486J.

Metzger, D.G., Loeltz, O.J., and Irelan, B., 1973, Geohydrology of the Parker-Blythe-Cibola area, Arizona and California: U.S. Geological Survey Professional Paper 486-G, 130 p., https://doi.org/10.3133/pp486G.

Moucha, R., Forte, A.M., Rowley, D.B., Mitrovica, J.X., Simmons, N.A., and Grand, S.P., 2008, Mantle convection and the recent evolution of the Colorado Plateau: Geology, v. 36, p. 439–442, https://doi.org/10.1130/G24577A.1.

Moucha, R., Forte, A.M., Rowley, D.B., Mitrovica, J.X., Simmons, N.A., and Grand, S.P., 2009, Deep mantle forces and the uplift of the Colorado Plateau: Geophysical Research Letters, v. 36, no. L19310, https://doi.org/10.1029/2009GL039778.

O'Connell, B., Dorsey, R.J., and Humphreys, E.D., 2017, Tidal rhythmites in the southern Bouse Formation as evidence for post-Miocene uplift of the lower Colorado River corridor: Geology, v. 45, p. 99–102, https://doi.org/10.1130/G38608.1.

O'Connell, B., Dorsey, R.J., Hasiotis, S.T., and Hood, A.V.S., 2020, Mixed carbonate-siliciclastic tidal sedimentation in the Miocene to Pliocene Bouse Formation, palaeo-Gulf of California: Sedimentology, v. 68, p. 1028–1068, https://doi.org/10.1111/sed.12817.

Pearthree, P.A., and House, P.K., 2014, Paleogeomorphology and evolution of the early Colorado River inferred from relationships in Mohave and Cottonwood valleys, Arizona, California, and Nevada: Geosphere, v. 10, p. 1139–1160, https://doi.org/10.1130/GES00988.1.

Porter, R., Hoisch, T., and Holt, W.E., 2017, The role of lower-crustal hydration in the tectonic evolution of the Colorado Plateau: Tectonophysics, v. 712–713, p. 221–231, https://doi.org/10.1016/j.tecto.2017.05.025.

Poulson, S.R., and John, B.E., 2003, Stable isotope and trace element geochemistry of the basal Bouse Formation carbonate, southwestern United States: Implications for the Pliocene uplift history of the Colorado Plateau: Geological Society of America Bulletin, v. 115, p. 434–444, https://doi.org/10.1130/0016-7606(2003)115<0434:SIATEG>2.0.CO;2.

Press, W.H., Flannery, B.P., Teukolsky, S.A., and Vetterling, 1986, Numerical Recipes: The Art of Scientific Computing: London, Cambridge University Press, 818 p.

Raymo, M.E., Kozdon, R., Evans, D., Lisiecki, L., and Ford, H.L., 2018, The accuracy of mid-Pliocene $\delta^{18}O$-based ice volume and sea level reconstructions: Earth-Science Reviews, v. 177, p. 291–302, https://doi.org/10.1016/j.earscirev.2017.11.022.

Richard, S.M., 1993, Palinspastic reconstruction of southeastern California and southwestern Arizona for the middle Miocene: Tectonics, v. 12, p. 830–854, https://doi.org/10.1029/92TC02951.

Roskowski, J.A., Patchett, P.J., Spencer, J.E., Pearthree, P.A., Dettman, D.L., Faulds, J.E., and Reynolds, A.C., 2010, A late Miocene-early Pliocene chain of lakes fed by the Colorado River: Evidence from Sr, C, and O isotopes of the Bouse Formation and related units between Grand Canyon and the Gulf of California: Geological Society of America Bulletin, v. 122, p. 1625–1636, https://doi.org/10.1130/B30186.1.

Roy, M., Jordan, T.H., and Pederson, J., 2009, Colorado Plateau magmatism and uplift by warming of heterogeneous lithosphere: Nature, v. 459, p. 978–982, https://doi.org/10.1038/nature08052.

Sahagian, D., Proussevitch, A., and Carlson, W., 2002, Timing of Colorado Plateau uplift: Initial constraints from vesicular basalt-derived paleoelevations: Geology, v. 30, p. 807–810, https://doi.org/10.1130/0091-7613(2002)030<0807:TOCPUI>2.0.CO;2.

Sampei, Y., Matsumoto, E., Dettman, D.L., Tokuoka, T., and Abe, O., 2005, Paleosalinity in a brackish lake during the Holocene based on stable oxygen and carbon isotopes of shell carbonate in Nakaumi Lagoon, southwest Japan: Palaeogeography, Palaeoclimatology, Palaeoecology, v. 224, p. 352–366, https://doi.org/10.1016/j.palaeo.2005.04.020.

Sarna-Wojcicki, A.M., Deino, A.L., Fleck, R.J., McLaughlin, R.J., Wagner, D., Wan, E., Wahl, D., Hillhouse, J.W., and Perkins, M., 2011, Age, composition, and areal distribution of the Pliocene Lawlor Tuff, and three younger Pliocene tuffs, California and Nevada: Geosphere, v. 7, p. 599–628, https://doi.org/10.1130/GES00609.1.

Schoell, M., 1978, Stable isotope analyses on authigenic carbonates from Lake Van sediments and their possible bearing on the climate of the past 10,000 years, *in* Degens, E.T., and Kurtman, F., eds., The Geology of Lake Van: Ankara, Turkey, M.T.A. Press, p. 92–97.

Severinghaus, J., and Atwater, T., 1990, Cenozoic geometry and thermal state of the subducting slabs beneath western North America, *in* Wernicke, B.P., ed., Basin and Range Extensional Tectonics Near the Latitude of Las Vegas, Nevada: Geological Society of America Memoir 176, p. 1–22, https://doi.org/10.1130/MEM176-p1.

Sloss, L.L., 1988, Tectonic evolution of the craton in Phanerozoic time, *in* Sloss, L.L., ed., Sedimentary Cover—North American craton: Boulder, Colorado, Geological Society of America, Geology of North America, v. D-2, p. 25–51.

Smith, P.B., 1970, New evidence for a Pliocene marine embayment along the lower Colorado River area, California and Arizona: Geological Society of America Bulletin, v. 81, p. 1411–1420, https://doi.org/10.1130/0016-7606(1970)81[1411:NEFAPM]2.0.CO;2.

Spencer, J.E., 1994, A numerical assessment of slab strength during high- and low-angle subduction: Journal of Geophysical Research: Solid Earth, v. 99, p. 9227–9236, https://doi.org/10.1029/94JB00503.

Spencer, J.E., 1996, Uplift of the Colorado Plateau due to lithosphere attenuation during Laramide low-angle subduction: Journal of Geophysical Research: Solid Earth, v. 101, p. 13,595–13,609, https://doi.org/10.1029/96JB00818.

Spencer, J.E., and Patchett, P.J., 1997, Sr isotope evidence for a lacustrine origin for the upper Miocene to Pliocene Bouse Formation, lower Colorado River trough, and implications for timing of Colorado Plateau uplift: Geological Society of America Bulletin, v. 109, p. 767–778, https://doi.org/10.1130/0016-7606(1997)109<0767:SIEFAL>2.3.CO;2.

Spencer, J.E., and Pearthree, P.A., 2001, Headward erosion versus closed-basin spillover as alternative causes of Neogene capture of the ancestral Colorado River by the Gulf of California, *in* Young, R.A., and Spamer, E.E., eds., The Colorado River: Origin and Evolution: Grand Canyon, Arizona, USA, Grand Canyon Association, Monograph 12, p. 215–219.

Spencer, R.J., Baedecker, M.J., Eugster, H.P., Forester, R.M., Goldhaber, M.B., Jones, B.F., Kelts, K., McKenzie, J., Madsen, D.B., Rettig, S.L., Rubin, M., and Bowser, C.J., 1984, Great Salt Lake, and precursors, Utah: The last 30,000 years: Contributions to Mineralogy and Petrology, v. 86, p. 321–334, https://doi.org/10.1007/BF01187137.

Spencer, J.E., Pearthree, P.A., and House, P.K., 2008, An evaluation of the evolution of the latest Miocene to earliest Pliocene Bouse lake system in the lower Colorado River valley, southwestern USA, *in* Reheis, M.C., Hershler, R., and Miller, D.M., eds., Late Cenozoic Drainage History of the Southwestern Great Basin and Lower Colorado River Region: Geologic and Biotic Perspectives: Geological Society of America Special Paper 439, p. 375–390, https://doi.org/10.1130/2008.2439(17).

Spencer, J.E., Patchett, P.J., Pearthree, P.A., House, P.K., Sarna-Wojcicki, A.M., Wan, E., Roskowski, J.A., and Faulds, J.E., 2013, Review and analysis of the age and origin of the Pliocene Bouse Formation, lower Colorado River Valley, southwestern USA: Geosphere, v. 9, p. 444–459, https://doi.org/10.1130/GES00896.1.

Spencer, J.E., Ferguson, C.A., Johnson, B.J., Gehrels, G., Pecha, M., and Doe, M., 2015, A partial compilation and database of U-Pb geochronologic data and sample locations in Arizona and southeastern-most California: Tucson, Arizona, Arizona Geological Survey, Digital Information Series DI-46, 2 p.

Spencer, J.E., Constenius, K., and Bright, J., 2018, Evidence of a lacustrine origin for laminated marl of the Pliocene Bouse Formation, Milpitas Wash, Blythe Basin, lower Colorado River valley: Arizona Geological Survey Contributed Report CR-18-K, 33 p., http://repository.azgs.az.gov/uri_gin/azgs/dlio/1901&gt.

Stone, P., Howard, K.A., and Hamilton, W., 1983, Correlation of metamorphosed Paleozoic strata of the southeastern Mojave Desert region, California and Arizona: Geological Society of America Bulletin, v. 94, p. 1135–1147, https://doi.org/10.1130/0016-7606(1983)94<1135:COMPSO>2.0.CO;2.

Talbot, M.R., 1990, A review of palaeohydrological interpretation of carbon and oxygen isotopic ratios in primary lacustrine carbonates [Isotope Geosciences Section]: Chemical Geology, v. 80, p. 261–279.

Talbot, M.R., and Kelts, K., 1986, Primary and diagenetic carbonates in the anoxic sediments of Lake Bosumtwi, Ghana: Geology, v. 14, p. 912–916, https://doi.org/10.1130/0091-7613(1986)14<912:PADCIT>2.0.CO;2.

Teranes, J.L., McKenzie, J.A., Bernasconi, S.M., Lotter, A.F., and Strum, M., 1999, A study of oxygen isotopic fractionation during bio-induced calcite precipitation in eutrophic Baldeggersee, Switzerland: Geochimica et Cosmochimica Acta, v. 63, p. 1981–1989, https://doi.org/10.1016/S0016-7037(99)00049-6.

Thacker, J.O., Karlstrom, K.E., Crossey, L.J., Crow, R.S., Cassidy, C.E., Beard, L.S., Singleton, J.S., Strickland, E.D., Seymour, N.M., and Wyatt, M.R., 2020, Post–12 Ma deformation in the lower Colorado River corridor, southwestern USA: Implications for diffuse transtension and the Bouse Formation: Geosphere, v. 16, p. 111–135, https://doi.org/10.1130/GES02104.1.

Todd, T.N., 1976, Pliocene occurrence of the recent atherinid fish *colpichthys regis* in Arizona: Journal of Paleontology, v. 50, p. 462–466.

Tosdal, R.M., and Wooden, J.L., 2015, Construction of the Jurassic magmatic arc, southeast California and southwest Arizona, *in* Anderson, T.H., Didenko, A.N., Johnson, C.L., Khanchuk, A.I., and MacDonald, J.H., Jr., eds., Late Jurassic Margin of Laurasia—A Record of Faulting Accommodating Plate Rotation: Geological Society of America Special Paper 513, p. 189–221, https://doi.org/10.1130/2015.2513(04).

Trapote, M.C., Vegas-Vilarrúbia, T., López, P., Puche, E., Gomà, J., Buchaca, T., Cañellas-Boltà, N., Safont, E., Corella, J.P., and Rull, V., 2018, Modern sedimentary analogues and integrated monitoring to understand varve formation in the Mediterranean Lake Montcortès (Central Pyrenees, Spain): Palaeogeography, Palaeoclimatology, Palaeoecology, v. 496, p. 292–304, https://doi.org/10.1016/j.palaeo.2018.01.046.

van Wijk, J.W., Baldridge, W.S., van Hunen, J., Goes, S., Aster, R., Coblentz, D.D., Grand, S.P., and Ni, J., 2010, Small-scale convection at the edge of the Colorado Plateau: Implications for topography, magmatism, and evolution of Proterozoic lithosphere: Geology, v. 38, p. 611–614, https://doi.org/10.1130/G31031.1.

Walk, C.J., Karlstrom, K.E., Crow, R.S., and Heizler, M.T., 2019, Birth and evolution of the Virgin River fluvial system: ~1 km of post–5 Ma uplift of the western Colorado Plateau: Geosphere, v. 15, p. 759–782, https://doi.org/10.1130/GES02019.1.

Williams, G.E., 2000, Geological constraints on the Precambrian history of Earth's rotation and the Moon's orbit: Reviews of Geophysics, v. 38, p. 37–59, https://doi.org/10.1029/1999RG900016.

Winnick, M.J., and Caves, J.K., 2015, Oxygen isotope mass-balance constraints on Pliocene sea level and East Antarctic Ice Sheet stability: Geology, v. 43, p. 879–882, https://doi.org/10.1130/G36999.1.